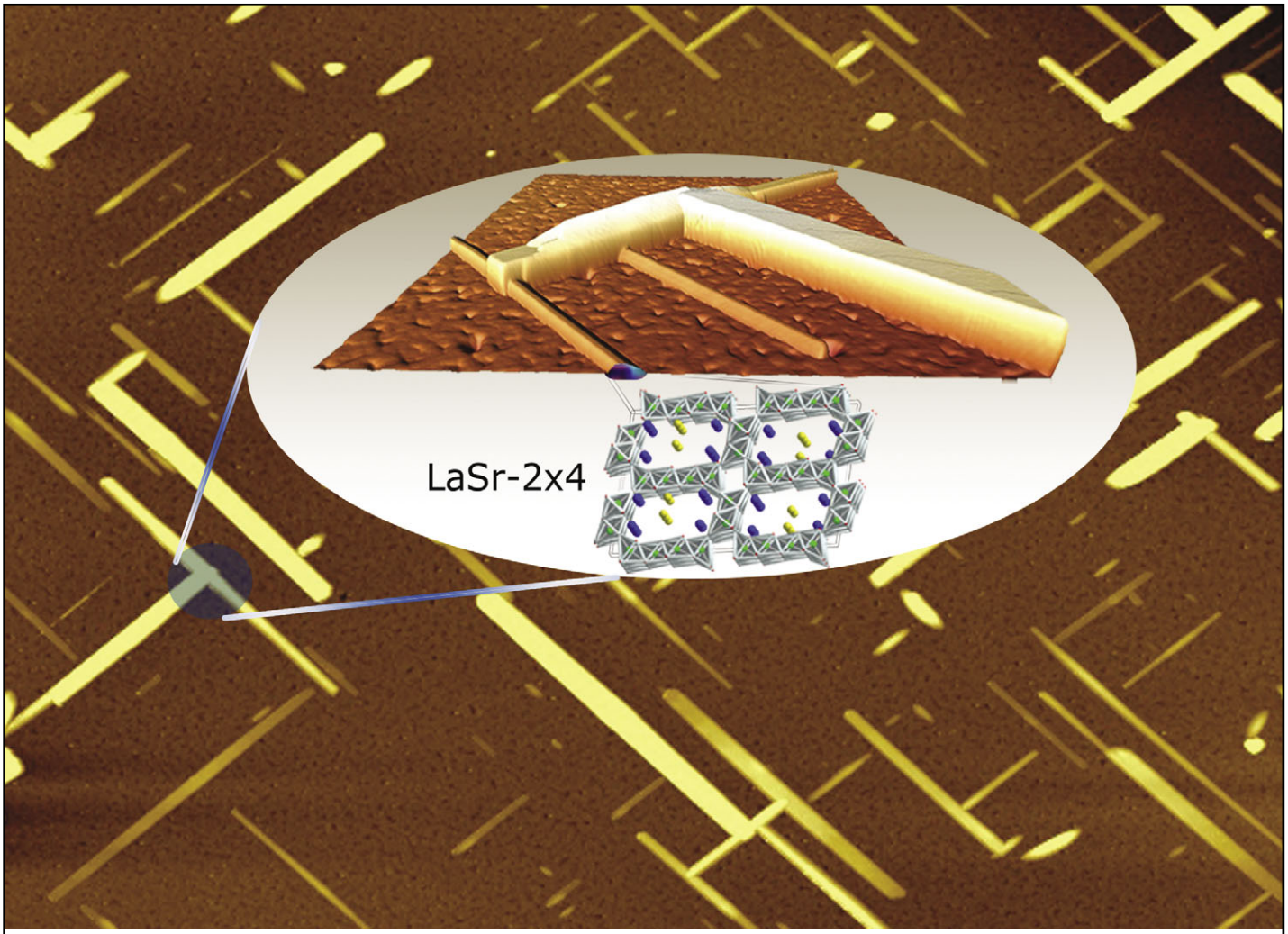

Showcasing research from the Institute of Materials Science of Barcelona, Consejo Superior de Investigaciones Científicas, Barcelona, Spain

Chemical synthesis of oriented ferromagnetic LaSr-2 × 4 manganese oxide molecular sieve nanowires

A new class of single crystalline LaSr-2 × 4 manganese oxide molecular sieve nanowires that are ferromagnetic at room temperature were grown epitaxially self aligned on fluorite type substrates by incorporating sol–gel based polymeric precursor solutions and track-etched polymer templates.

As featured in:

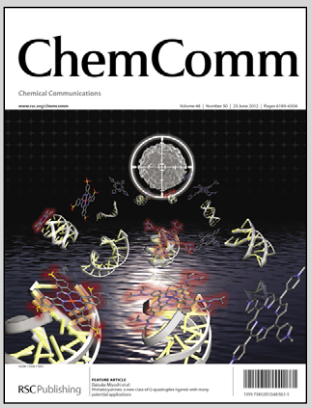

See N. Mestres *et al.*, *Chem. Commun.*, 2012, **48**, 6223.

RSC Publishing

www.rsc.org/chemcomm

Registered Charity Number 207890

ChemComm

Dynamic Article Links
View Article Online

Cite this: *Chem. Commun.*, 2012, **48**, 6223–6225

www.rsc.org/chemcomm

COMMUNICATION

Chemical synthesis of oriented ferromagnetic LaSr-2 × 4 manganese oxide molecular sieve nanowires†

Adrián Carretero-Genevrier,‡§[a] Jaume Gazquez,§¶[bc] César Magén,[d] María Varela,[cb] Etienne Ferain,[ef] Teresa Puig,[a] Narcís Mestres*[a] and Xavier Obradors[a]

Received 23rd February 2012, Accepted 24th April 2012
DOI: 10.1039/c2cc31367g

We report a chemical solution based method using nanoporous track-etched polymer templates for producing long and oriented LaSr-2 × 4 manganese oxide molecular sieve nanowires. Scanning transmission electron microscopy and electron energy loss spectroscopy analyses show that the nanowires are ferromagnetic at room temperature, single crystalline, epitaxially grown and self-aligned.

Due to their highly tuneable ground states, complex oxides exhibit a wide variety of different phenomena, such as high-T_c superconductivity in layered cuprates, colossal magnetoresistance in perovskite manganites, or coexistence of magnetism and ferroelectricity.[1,2] Nanoscale complex oxides display different magnetic, electrical, optical and mechanical properties compared to their bulk counterparts. Recently, investigations concerning their nanoscale characteristics, in particular one dimensional (1D) magnetic nanostructures, have received a great deal of attention for the development of future technologies like magnetic memories[3] or new types of sensors and logic devices based on magnetic oxides.[4–7] Planar nanowires (NWs) have been investigated because of their potential use in domain-wall devices proposed for data storage[8] and logic applications.[9] In this context, the large-scale assembly of NWs with controlled orientation on surfaces remains one challenge preventing integration into practical devices.

Although the epitaxial growth of horizontally aligned NWs has been recently reported for a limited number of simple oxides[10,11] and semiconductor materials using the vapour–liquid–solid growth method,[12–14] a new approach is needed for multi-component oxide materials due to the absence of appropriate catalysts and to the difficulties in controlling the reaction and achieving stoichiometry at the nanoscale. We have recently established a novel and general methodology to prepare complex oxides nanostructures by incorporating sol–gel based polymeric precursor solutions and track-etched polymer templates. Because of the confined nucleation in high aspect ratio nanopores and the high temperatures attained, different structural configurations with distinct physical properties were obtained as a function of the single crystal substrate used and the thermal treatment.[15–17] Our particular growth method has allowed the synthesis of monoclinic ferromagnetic single crystalline molecular sieve LaSr-2 × 4 manganese oxide NWs with enhanced Curie temperature (T_c > 500 K).[15,17] We demonstrate that our novel approach, using nanoporous track-etched polymer templates and a proper selection of process conditions and heteroepitaxial strain control, is able to produce 1D LaSr-2 × 4 manganese oxide molecular sieve NWs that are self-aligned and epitaxially grown on stable (001)-$Ce_{1-x}Gd_xO_{2-y}$ (CGO) fluorite substrates.

(001)-Oriented CGO buffer thin films were first grown on top of (001)-yttria stabilized ZrO_2 (YSZ) substrates by chemical solution deposition.[18,19] The CGO buffer layers grow cube on cube with excellent epitaxial quality on top of the YSZ substrate (Fig. S1, ESI†). For the nanowires growth, we followed the same growth method described elsewhere.[17] Briefly, supported nanoporous polycarbonate (PC) films were defined on top of the CGO buffer thin films. The supported nanoporous templates were filled by capillary force using a sol–gel based polymer precursor solution of $La_{0.7}Sr_{0.3}MnO_3$ (LSMO); the specimens were heated in a furnace at temperatures 700−1000 °C for 30 min to 10 hours in a pure oxygen atmosphere. During this process the PC polymer (with a decomposition temperature in a single step between 400 and 500 °C) is consequently pyrolysed.

A thermal treatment at 1000 °C resulted in continuous and long nanowires. The field emission scanning electron microscopy (FESEM) image of Fig. 1a shows that these NWs grew straight on the (001)-CGO surface and aligned along two orthogonal directions parallel to the [110] and [1$\bar{1}$0] directions of the CGO substrate. This observation can be further confirmed from the 2D fast Fourier transform (FFT) (Fig. 1a, inset), where two high intensity lines separated by 90° are clearly evident, thus indicating

[a] *Institut de Ciència de Materials de Barcelona ICMAB, CSIC, Campus UAB 08193 Bellaterra, Catalonia, Spain. E-mail: narcis.mestres@icmab.es*
[b] *Departamento de Física Aplicada III, Universidad Complutense de Madrid, Madrid, 28040, Spain*
[c] *Materials Science and Technology Division, Oak Ridge National Laboratory, Oak Ridge, TN 37831, USA*
[d] *Laboratorio de Microscopías Avanzadas LMA—Instituto de Nanociencia de Aragón INA-ARAID Universidad de Zaragoza, 50018 Zaragoza, Spain*
[e] *Institute of Condensed Matter and Nanosciences, Bio & Soft Matter (IMCN/BSMA), Université catholique de Louvain, Croix du Sud 1, 1348 Louvain-la-Neuve, Belgium*
[f] *it4ip s.a, 7180 Seneffe, Belgium*

† Electronic supplementary information (ESI) available: Details of synthesis and characterization. See DOI: 10.1039/c2cc31367g

‡ Present address: Laboratoire de Chimie de la Matière Condensée de Paris, UMR7574, 75231 Paris cedex 05, France.
§ Adrián Carretero-Genevrier and Jaume Gazquez contributed equally to this work.
¶ Present address: Institut de Ciència de Materials de Barcelona ICMAB, CSIC, Campus UAB 08193 Bellaterra, Catalonia, Spain.

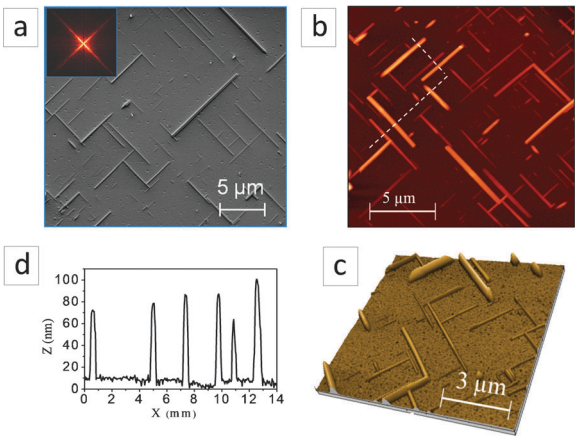

Fig. 1 (a) FESEM image revealing the formation of nanowires and its preferential growth directions parallel to the [110] and [$\bar{1}$10] directions of the (001)-CGO substrate. The inset shows the 2D fast Fourier transform (FFT). (b) and (c) 2D and 3D AFM images, respectively, of self-assembled nanowires together with the AFM profile analysis (d).

the existence of long range ordering of NWs along two specific perpendicular directions. The length of the NWs can be controlled with increasing the growth time. After a growth time of 10 hours their length may reach several tens of micrometers (Fig. S4, ESI†). Representative AFM images are given in Fig. 1b and c. The top surface and the edges of the NWs were very regular and uniform in height and width over their entire length. Using the same growth procedure we did not observe the horizontal oriented NWs on (001)-Si,[17] (001)-LAO and (001)-STO[16] substrates, demonstrating the important role of the substrate crystallographic plane in determining the NWs self-assembly and orientation.

X-ray diffraction measurements confirmed that the self-assembled NWs on top of (001)-CGO substrates had the monoclinic unit cell recently reported for LaSr-2 × 4 free-standing ferromagnetic nanowires[17] and the epitaxial relation existing with the CGO substrate. Measurements were performed using a two dimensional X-ray detector (XRD2). Fig. 2(a) displays the pole figure for $2\theta = 26.8°$ with the reflections at $\chi = 12.6°$ and $\chi = 40.0°$ corresponding to LaSr-2 × 4 NWs, and the four reflections at $\chi = 54.0°$ related to the CGO substrate. The results of different pole figures are schematically summarized in Fig. 2(b). The four poles, larger peaks (brown dots), observed at $\chi = 54°$ and oriented at φ values separated by 90° indicate the (001) oriented CGO thin film on top of the (001)-YSZ single-crystal substrate. The fainter peaks observed at different χ and ϕ positions correspond to the different poles of the LaSr-2 × 4 monoclinic unit cell orientation on top of the (001)-CGO thin film. Those from the experimental data are displayed in red, while theoretical reflection's positions are displayed in blue. Detailed peak assignment can be found in Table S1 (ESI†).

A dedicated STEM VG Microscope HB501UX equipped with an Enfina EEL spectrometer and a NION aberration corrector operated at 100 kV was used to confirm the epitaxial growth of these LaSr-2 × 4 single crystal NWs on the CGO substrate. Scanning transmission electron microscopy (STEM) characterization was performed by preparing a cross section of self-assembled NWs, thus allowing looking at the epitaxial NWs substrate interface from a side view. Fig. 3a displays an annular dark field (ADF) Z-contrast image of one single

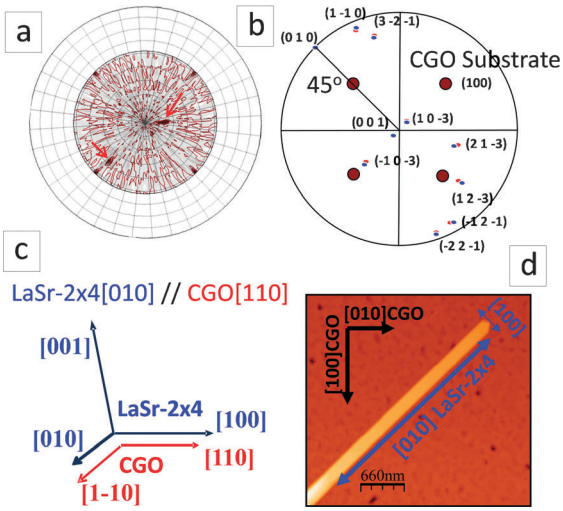

Fig. 2 (a) Pole figure for $2\theta = 26.8°$, peaks observed at $\chi = 12.6°$ and $\chi = 40.0°$ (see arrows) correspond to LaSr-2 × 4 NWs and the four peaks at $\chi = 54.0°$ correspond to the CGO substrate. (b) XRD2 simulation of LaSr-2 × 4 NWs grown on CGO substrates. Brown circles show the {001}CGO poles, red and blue circles represent experimental and theoretical reflections of the monoclinic LaSr-2 × 4 NWs (c), (d) AFM image with the schematic representation of the orientation for a LaSr-2 × 4 NW.

LaSr-2 × 4 NW cut perpendicular to its long axis lying on the CGO buffer layer. This specific NW is about 100 nm wide and 100 nm high. Fig. 3b shows a LaSr-2 × 4 NW with the epitaxial relation LSMO[010]//CGO[1$\bar{1}$0] viewed along the [30$\bar{1}$]-zone axis. The indexed FFT spectrum in the inset of Fig. 3b indeed reveals diffraction spots from (020) and (206) LaSr-2 × 4 lattice fringes. STEM in combination with electron

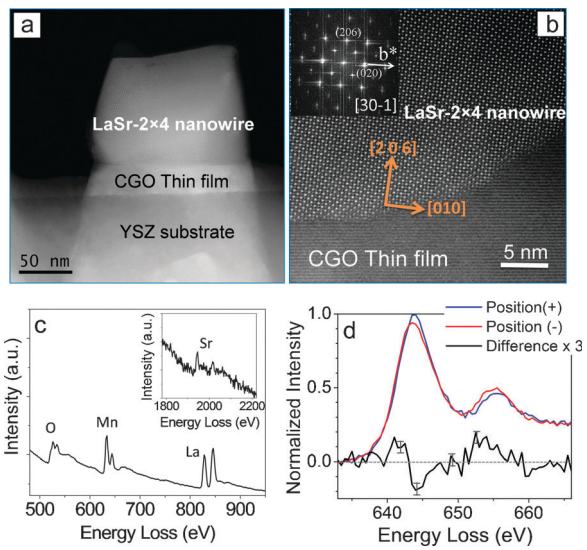

Fig. 3 (a) Low resolution ADF image of one single-crystal LaSr-2 × 4 nanowire grown at 1000 °C. (b) High resolution ADF Z-contrast image of the interface between an epitaxial LaSr-2 × 4 nanowire oriented LSMO [010]||CGO [1$\bar{1}$0] and the CGO buffer layer, viewed along [30$\bar{1}$]. The inset shows the corresponding FFT. (c) EEL spectrum generated from the EELS scans across the nanowire displayed in (a). (d) Mn $L_{2,3}$ edges in the two configurations (+) and (−), the difference is 0.06, and has been magnified by a factor of 3 in the figure. The r.m.s. of the noise, indicated by the error bars is ±15% of the difference.

energy loss spectroscopy (EELS) allowed us to explore the chemistry and identify the main elements of the NWs. Fig. 3c shows the EEL spectrum generated from the EELS scans across the nanowire displayed in Fig. 3a and confirms that the NWs are composed of La, Sr, Mn and O and that the composition is uniform along the wires with no impurities present.

Hence, both the STEM and the diffraction data prove that the LaSr-2 × 4 NWs grew epitaxially on top of the CGO buffered YSZ substrate with a well defined crystalline orientation and had the monoclinic unit cell already reported for LaSr-2 × 4 molecular sieve nanowires.[17] They constitute a new type of Mn oxides characterized by tunnels that measure 2 and 4 MnO_6 octahedra with arrangement of Sr^{2+} and La^{3+} cations inside the channels. Other complex functional oxides may lead to new cationic arrangements inside the tunnels with modified physical properties. We consider that the large intrinsic anisotropy of the monoclinic LaSr-2 × 4 structure is what promotes the 1D growth along the NWs [010] direction (the direction of smallest interplanar distance). This fact combined with the low isotropic residual misfit along the ⟨110⟩ CGO directions (a residual misfit of 0.74% is estimated along both directions (Fig. S3, ESI†)) permitted the self-assembly of LaSr-2 × 4 NWs along these directions. Although the surface energies for the monoclinic LaSr-2 × 4 crystallographic structure are not known at this moment, the minimization of the surface energy by maximizing the area of the lower energy facets must play a relevant role in the 1D-growth and has to be elucidated in future studies.

The low scale of the system made it impossible to perform the magnetic characterization of these NWs by means of superconducting quantum interference device (SQUID) magnetometry. Still, the magnetism of these NWs has been proved using EELS in a FEI Titan 60–300 microscope equipped with a X-FEG gun, a CETCOR probe corrector and a Gatan energy filter TRIDIEM 866 ERS operated in STEM at 300 kV. As has recently been shown by Schattschneider *et al.*,[20] energy-loss magnetic chiral dichroism (EMCD) can be measured in a TEM studying $L_{2,3}$ EELS absorption edges of transition metals. Following the procedures described by the authors, we have obtained the two Mn $L_{2,3}$ edges from two conjugated spots in the nanodiffraction diagram (equivalent to the two beam polarizations used in X-ray magnetic circular dichroism measurements), see Fig. 3d. The dichroic signal is then given by the difference between these two spectra (see ESI† for full experimental details). Further evidence comes from calculating the L_3/L_2 ratio for each spectrum, which using the 2nd derivative method gives (4.3 ± 0.1) and (3.5 ± 0.1) for positions (+) and (−), respectively. A very similar dichroic signal was measured in the free-standing NWs of ref. 17. The previous EMCD experiment has been performed at room temperature, therefore the epitaxial LaSr-2 × 4 NWs are proved to be ferromagnetic at least up to 300 K.

We have demonstrated a versatile approach towards the controlled epitaxial growth of self-aligned LaSr-2 × 4 NWs on the (001)-CGO surface, combining solution chemistry with nanoporous polymer templates coating CGO substrates. We have verified by means of XRD and TEM analyses in combination with EELS that at high growth temperatures ($T_g \geq 800$ °C) single crystalline LaSr-2 × 4 monoclinic NWs are formed, that are ferromagnetic at room temperature, and that grow epitaxially with the [010] nanowire's longitudinal axis parallel to the [110] and [1$\bar{1}$0] directions of the CGO substrate. Due to their ferromagnetic behavior and to the resulting planar geometry, these nanowires are very appealing for potential technological applications in data storage and in spintronic devices. This new procedure provides a successful example of self-organization processes that use nanoporous track-etched polymer templates as nanoreactors together with the correct substrate choice for the controlled fabrication of ordered arrays of nanowires on single crystal surfaces. Considering the novel outstanding magnetic properties and the efficient methodology used to generate these nanowires, we are convinced that our approach will become an extremely appealing route towards the generation of epitaxial self-assembled functional oxide nanowires.

We acknowledge the financial support from MICINN (MAT2008-01022, Consolider NANOSELECT CSD 2007-00042, and FPI), EU (HIPERCHEM, NMP4-CT2005-516858) and Generalitat de Catalunya (SGR 770 and XaRMAE). Work at ORNL was supported by the Office of Science, Materials Sciences and Engineering Division of the US Department of Energy (M.V.). J.G. is thankful for financial support from the ERC, grant #239739 STEMOX.

Notes and references

1 S. Cheong and M. Mostovoy, *Nat. Mater.*, 2007, **6**, 13.
2 R. Ramesh and N. A. Spaldin, *Nat. Mater.*, 2007, **6**, 21.
3 S. Yamanaka, T. Kanki, T. Kawai and H. Tanaka, *Nano Lett.*, 2011, **11**, 343.
4 C. H. Kim, Y. Myung, Y. J. Cho, H. S. Kim, S. Park, J. Park, J. Kim and B. Kim, *J. Phys. Chem. C*, 2009, **113**, 7085.
5 K. R. Bhayani, S. N. Kale, S. Arora, R. Rajagopal, H. Mamgain, R. Kaul-Ghanekar, D. C. Kundaliya, S. D. Kulkarni, R. Pasricha, S. D. Dhole, S. B. Ogale and K. M. Paknikar, *Nanotechnology*, 2007, **18**, 345101.
6 K. Goto, H. Tanaka and T. Kawai, *Nano Lett.*, 2009, **9**, 1962.
7 S. Han, C. Li, Z. Liu, B. Lei, D. Zhang, W. Jin, X. Liu, T. Tang and C. Zhou, *Nano Lett.*, 2004, **4**, 1241.
8 M. Hayashi, L. Thomas, R. Moriya, C. Rettner and S. S. P. Parkin, *Science*, 2008, **320**, 209.
9 D. A. Allwood, G. Xiong, C. C. Faulkner, D. Atkinson, D. Petit and R. P. Cowburn, *Science*, 2005, **309**, 1688.
10 M. Gibert, P. Abellán, A. Benedetti, T. Puig, F. Sandiumenge, A. García and X. Obradors, *Small*, 2010, **6**, 2716.
11 K. H. L. Zhang, A. Walsh, C. R. A. Catlow, V. K. Lazarov and R. G. Egdell, *Nano Lett.*, 2010, **10**, 3740.
12 B. Nikoobakht, C. A. Michaels, S. J. Stranick and M. D. Vaudin, *Appl. Phys. Lett.*, 2004, **85**, 3244.
13 S. A. Fortuna, J. Wen, I. S. Chun and X. Li, *Nano Lett.*, 2008, **8**, 4421.
14 D. Tsivion, M. Schvartzman, R. Popovitz-Biro, P. von Huth and E. Joselevich, *Science*, 2011, **333**, 1003.
15 A. Carretero-Genevrier, N. Mestres, T. Puig, A. Hassini, J. Oro, A. Pomar, F. Sandiumenge, X. Obradors and E. Ferain, *Adv. Mater.*, 2008, **20**, 3672.
16 A. Carretero-Genevrier, J. Gázquez, T. Puig, N. Mestres, F. Sandiumenge, X. Obradors and E. Ferain, *Adv. Funct. Mater.*, 2010, **20**, 2139.
17 A. Carretero-Genevrier, J. Gázquez, J. C. Idrobo, J. Oró, J. Arbiol, M. Varela, E. Ferain, J. Rodríguez-Carvajal, T. Puig, N. Mestres and X. Obradors, *J. Am. Chem. Soc.*, 2011, **133**, 4053.
18 A. Cavallaro, F. Sandiumenge, J. Gàzquez, T. Puig, X. Obradors, J. Arbiol and H. Freyhardt, *Adv. Funct. Mater.*, 2006, **16**, 1363.
19 M. Coll, J. Gázquez, F. Sandiumenge, T. Puig, X. Obradors, J. P. Espinós and R. Hühne, *Nanotechnology*, 2008, **19**, 395601.
20 P. Schattschneider, S. Rubino, C. Hebert, J. Rusz, J. Kunes, P. Novák, E. Carlino, M. Fabrizioli, G. Panaccione and G. Rossi, *Nature*, 2006, **441**, 486.